HHS Public Access

Author manuscript

Biomater Sci. Author manuscript; available in PMC 2022 March 10.

Published in final edited form as:

Biomater Sci. 2020 July 21; 8(14): 3804–3811. doi:10.1039/d0bm00860e.

Viscoelasticity of hydrazone crosslinked poly(ethylene glycol) hydrogels directs chondrocyte morphology during mechanical deformation

Benjamin M. Richardson[a,b], **Cierra J. Walker**[b,c], **Laura J. Macdougall**[b], **Jack W. Hoye**[a], **Mark A. Randolph**[d,e], **Stephanie J. Bryant**[a,b,c], **Kristi S. Anseth**[a,b]

[a]Department of Chemical and Biological Engineering, University of Colorado Boulder, 3415 Colorado Ave, Boulder, CO 80303, USA.

[b]The BioFrontiers Institute, University of Colorado Boulder, 3415 Colorado Ave, Boulder, CO 80303, USA.

[c]Materials Science and Engineering Program, University of Colorado Boulder, 4001 Discovery Drive, Boulder, CO 80303, USA

[d]Department of Orthopedic Surgery, Massachusetts General Hospital, Harvard Medical School, 55 Fruit St, WAC 435, Boston, MA 02114, USA

[e]Division of Plastic Surgery, Massachusetts General Hospital, Harvard Medical School, 15 Parkman St, WACC 453, Boston, MA 02114, USA

Abstract

Chondrocyte deformation influences disease progression and tissue regeneration in load-bearing joints. In this work, we found that viscoelasticity of dynamic covalent crosslinks temporally modulates the biophysical transmission of physiologically relevant compressive strains to encapsulated chondrocytes. Chondrocytes in viscoelastic alky-hydrazone hydrogels demonstrated (91.4 ± 4.5%) recovery of native rounded morphologies during mechanical deformation, whereas primarily elastic benzyl-hydrazone hydrogels significantly limited morphological recovery (21.2 ± 1.4%).

Graphical Abstract

Viscoelasticity of dynamic covalent crosslinks temporally modulates the biophysical transmission of physiologically relevant compressive strains to encapsulated chondrocytes

† benjamin.richardson@colorado.edu, kristi.anseth@colorado.edu.

Conflicts of Interest

The authors declare no competing financial interests.

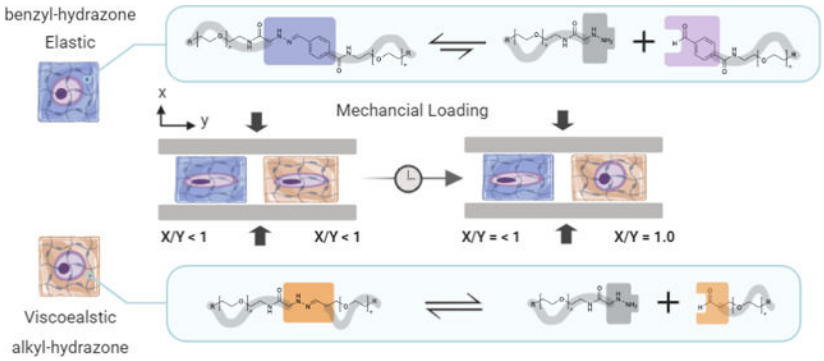

Symptomatic knee osteoarthritis is estimated to affect nearly 1 in 5 Americans over the age of 45.[1] These patients experience chronic pain caused by damage to articular cartilage in load-bearing joints.[2] Degeneration of articular cartilage during the onset of osteoarthritis is typically compounded by the avascular structure and the limited regenerative capacity of resident chondrocytes.[3] Fortunately, tissue engineering strategies such as matrix-assisted autologous chondrocyte transplantation (MACT) have been developed to augment chondrocyte's natural ability to regenerate during disease progression.[4] This strategy involves using water-swollen polymer networks, to support chondrocyte growth, enhance their regenerative capacity and deliver cells to the defect site.[5] To withstand compressive forces experienced in articulating joints, hydrogels developed for cartilage tissue engineering are often covalently crosslinked. However, traditional covalent crosslinks lead to an elastic response to mechanical deformation. In addition, non-degradable covalent crosslinks can limit chondrocyte proliferation and extracellular matrix (ECM) deposition.[6] These limitations may suggest an explanation for why MACT remains an uncommon clinical treatment relative to microfracture.[7]

To improve regenerative outcomes of MACT, hydrogels can be designed with viscoelastic properties, making them more similar to the ECM chondrocytes experience *in vivo*.[8,9] More specifically, freshly isolated cartilage tissue demonstrates viscoelastic matrix properties, such as stress relaxation and creep in addition to poroelastic interstitial fluid flow.[10] While covalently crosslinked hydrogels used as chondrocyte matrices allow for robust tuning of the elastic modulus of the material, they do not demonstrate time dependent material properties during mechanical deformation and permanent crosslinks can inhibit tissue regeneration.[11] Few cartilage regeneration studies have investigated how viscous dissipation (*e.g.,* stress relaxation and material creep) influence chondrocyte deformation by comparison with the more well-studied effects of elastic stiffness.[12,13] Furthermore, many previously studied viscoelastic networks rely on electrostatic interactions (e.g., calcium-alginate) or entanglement (e.g., collagen) resulting in lower moduli than analogous covalently crosslinked hydrogels potentially limiting their ability to withstand compressive loading in articulating joints.[8] As a complement to existing hydrogels used for chondrocyte encapsulation, covalent adaptable networks (CANs) are a rapidly growing class of biomaterials.[14] When synthesized from water soluble precursors under physiological conditions, reversible covalent crosslinks offer both robust mechanical support and

viscoelastic network reorganization uniquely suited for cartilage tissue engineering in compression bioreactors (*in vitro*) or in load bearing joints (*in vivo*).[15]

In recent work, dynamic covalent chemistries (e.g., Diels-Alder reactions, Schiff bases, hydrazones, oximes and boronate esters) have been applied as CAN scaffolds for cell encapsulation and tissue engineering.[16,17] Related to this study, hydrazone CANs in particular can be used to encapsulate primary cells due to mild formation conditions (pH 7.0, 25°C) without a catalyst.[18,19] Hydrazone bonds (R-HC=NH-NH-R) are formed when a nucleophilic hydrazine or hydrazide attacks a carbonyl electrophile in a condensation reaction, producing water as the only byproduct.[20] These hydrazone bonds are also susceptible to hydrolysis, rendering the process reversible.[21] Natural chemical equilibria, or the balance between these forward and reverse reactions is responsible for the viscoelastic network reorganization of hydrazone CANs. For example, adjacent electron withdrawing groups (e.g., benzene rings) can be used to stabilize hydrazone bonds.[21] The increased hydrolytic stability of benzyl-hydrazone bonds relative to alkyl-hydrazone bonds (i.e. smaller reverse rate constant) leads to slower covalent crosslink adaptation and more elastic (i.e. less viscoelastic) material behavior.[18] This phenomena has been verified by small molecule kinetic studies showing that rate constants measured by small molecule kinetic studies can be used to understand the viscoelastic material properties of hydrazone CANs.[22] The dynamic nature of hydrazone crosslinks makes them especially attractive as extracellular matrix mimics for tissue engineering.[23,24]

In this work, poly(ethylene glycol) (PEG) macromers were functionalized with nucleophilic hydrazines and electrophilic aldehydes. PEG is an attractive material because it is biologically inert and easy to modify. These characteristics minimize non-specific protein interactions and circumvent biochemical cues from naturally derived polymers which could confound studies aiming to elucidate biophysical effects of viscoelasticity.[25] The average functionalization of each type of PEG macromer was estimated (Table S1) using integrations for distinct functional groups normalized by PEG protons. (Fig. S1) In each case the functionalization was found to be >80%. Reactive components were mixed off-stoichiometry (r = 0.8) to engineer hydrogels with user defined control over the viscoelastic properties by varying the molar percentages of alkyl-hydrazone and benzyl-hydrazone dynamic covalent crosslinks. Three hydrogel formulations were tested by shear rheology to investigate the accessible range of viscoelastic properties. (Fig. 1) Formulations represent a viscoelastic 100% alkyl-hydrazone (0% benzyl-hydrazone) an elastic 0% alkyl-hydrazone (100% benzyl-hydrazone) as well as an optimized mixed condition, 78% alkyl-hydrazone (22% benzyl-hydrazone).[26] These hydrogel formulations were selected to yield a similar shear moduli (G) and remove stiffness as a confounding variable. (Fig. 1A) This is an important characteristic to control, as crosslinking density has been previously shown to influence chondrocyte morphology during deformation.[27] Hydrogel stiffness was selected to approximate the stiffness of encapsulated chondrocytes.[28]. Importantly, despite matched stiffness, these hydrogels maintained differences in loss tangents $\tan(\delta) = G''/G'$, illustrating differences in the viscous and elastic contributions to the shear modulus. (Fig. 1D)

Viscoelastic properties were measured through stress relaxation and creep tests to investigate how equilibrium differences of hydrazone crosslinks alter the scaffold response to

deformation. Stress relaxation tests (Fig. 1B) were comparable with previous results, exhibiting average relaxation times (Fig. 1E) from (7.20 ± 1.1 1) x 10^3 s to (1.42 ± 0.06) x 10^6 s based on the Kohlrausch–Williams–Watts stretched exponential function.[26] (Eq. S3 & S4) More interestingly, these networks also exhibited material deformation, or creep, in response to a constant shear stress. (Fig. 1C) These differences were quantified by linear fitting, (Eq. S5) excluding creep ring artifacts and illustrating significant differences from (5.19 ± 0.54) x 10^{-7} $Pa^{-1}s^{-1}$ to (9.59 ± 2.78) x 10^{-9} $Pa^{-1}s^{-1}$. (Fig. 1F) This treatment is consistent with the physical representation of the stretched exponential used to model stress relaxation and would be representative of an aggregate creep rate due to an infinite series of Maxwell elements in parallel.[29] (Fig. S2) Importantly, all three formulations result in non-significantly different shear moduli, which is directly proportional to the crosslink density.[30] Additionally, the average functionalization and polymer content are approximately equal between formulations. Therefore it is reasonable to assume that any differences in crosslinking efficiency are negligible and that differences in viscoelasticity can be attributed to bond dynamics of alkyl-hydrazone and benzyl-hydrazone crosslinks.

Armed with a better understanding of how these hydrogels respond to mechanical deformation, we sought to examine how differences in viscoelastic properties of hydrazone CANs would influence the morphology of encapsulated chondrocytes during mechanical deformation. (Fig. 2) To accomplish this, porcine chondrocytes were stained with CellTracker™ Orange, encapsulated in cuboid hydrogels, and imaged *in situ* by confocal microscopy. (Fig. 2A) Representative maximum intensity projections of single chondrocytes exposed to a 20% uniaxial compressive strain illustrate changes in chondrocyte morphology over 10 hours due to viscoelasticity. (Fig. 2C) These qualitative changes in chondrocyte morphology were then quantified by measuring the cell deformation index.[31] The deformation index (Fig. 2B & Fig. 2D) was calculated as the quotient of the cell dimension parallel to the axis of compression (X) and the cell dimension perpendicular to the axis of compression (Y).[32] Previously, we have observed that a 20% macroscopic strain corresponded to X/Y = 0.8 ± 0.1 in PEG hydrogels with low crosslinking densities, which is higher than would be expected (X/Y = 0.67) assuming cell volume remains constant.[33,34] Initially, this was observed in all three conditions, with unstrained deformation indices close to 1.0 followed by cellular deformation to approximately 0.8 immediately after application of a 20% compressive strain. (Fig. S4) However, after 10 hours of applied strain, the morphologies of chondrocytes in the highly viscoelastic 100% alkyl hydrazone hydrogels and the primarily elastic 0% alkyl hydrazone hydrogels diverge significantly. During 10 hours of deformation at 20% strain, chondrocytes encapsulated in the viscoelastic 100% adaptable hydrogels recovered their unstrained rounded morphologies. (X/Y = 0.97 ± 0.03) Whereas, chondrocytes in the elastic 0% adaptable hydrogels largely retained deformed ellipsoidal morphologies (X/Y = 0.86 ± 0.05).

For the morphology of an encapsulated chondrocyte to change within these 3D hydrogel matrices, the network crosslinks must be able to transmit strain to the cellular level. Similarly, for a chondrocyte to recover a rounded morphology while under deformation, the cell must exert a stress on the network and the crosslinks must rearrange or creep to allow the cell to change shape.[35] Therefore, it follows that creep compliance would be the viscoelastic behavior driving changes in chondrocyte morphology in hydrazone CANs

during mechanical deformation. Graphing the cellular deformation index after 10 hours of deformation by the linear creep rate reveals a linear correlation, which is consistent with the rheological understanding that the material must creep to allow the cell morphology to change. (Fig 2D) This cellular observation is particularly interesting in comparison with the macroscopic dimensions of the hydrogels before and after 10 hours of deformation at 20% strain. (Fig 2E) The viscoelastic 100% hydrogel macroscopically creeped to adopt the deformed shape even after the load was removed. In contrast, the 0% hydrogels elastically retained similar dimensions before and after strain removal. As expected, the hybrid 78% condition exhibited behavior between the two extremes fitting the intermediate creep rate measured by shear rheology. Notably, the trend for bulk hydrogel deformation (L_x/L_y) after strain removal was inverse of the cellular deformation (X/Y) during deformation, illustrating consistent creep compliance behaviour at both the microscopic and macroscopic length scales.

To further investigate the biophysical transmission of mechanical strain to encapsulated chondrocytes, we sought to track morphology changes over time. This allowed us to map the influence of viscoelasticity on cell-matrix interactions in hydrazone CANs. (Fig. 3) Chondrocytes in the most adaptable 100% condition rapidly regained rounded morphologies, becoming non-significantly different from the unstrained chondrocytes after only 5 hours. (Fig. 3A & 3B) Material testing by shear rheology indicates that after 5 hours the network should have been able to relax >80% of an applied strain. This implies that a large fraction of the pericellular crosslinks must rearrange in order to influence chondrocyte morphology in hydrazone CANs. Furthermore, chondrocytes encapsulated in the viscoelastic 100% CAN hydrogels continued to approach their initial spherical morphologies over the course of the experiment, eventually showing 91.4 ± 4.5% recovery. (Eq. S6) This phenomena is consistent with that observed in viscoelastic alginate hydrogels, where chondrocytes experience a decrease in cellular strain over time in low polymer content ionically crosslinked hydrogels.[36]

Similarly, the 78% condition demonstrated viscoelastic recovery, albeit over a much slower time scale. Chondrocyte morphologies became less significantly different from the initial unstrained state over the course of the deformation period. (Fig. 2C & 2D) This is also consistent with the theoretical framework, as 22% benzyl-hydrazone crosslinks (78% alkyl-hydrazone) is above the Flory-Stockmayer percolation threshold. Meaning the hybrid hydrogels are composed of an interconnected network with both alkyl-hydrazone and benzyl-hydrazone crosslinks spanning the dimensions of the hydrogel.[37] (Eq. S1) Therefore, the behavior of chondrocytes in the 78% condition can be understood to be influenced by competing elastic and viscoelastic crosslinks. The result of this is partial recovery of the rounded morphology during deformation, followed by full elastic recovery in the wake of strain removal. Importantly, this shows that incorporating a relatively small percentage of benzyl-hydrazone crosslinks (22 mol %) can significantly impact network reorganization which in turn influences cellular morphology during deformation. (e.g., 32.7 ± 1.7% recovery)

In accordance with prior results, the 0% hydrogels behaved as ideal elastic solids, maintaining statistically significant chondrocyte deformation over the entire 10 hour strain

period. Chondrocytes in the 0% condition showed limited recovery during deformation, (21.2 ± 1.4%) followed by instantaneous recovery when the 20% strain was removed (Fig. 3E–F). We had postulated that this would be the case due to the short experimental time relative to the average relaxation time for 0% networks (10^4 s << 10^6 s). The elastic response of the 0% hydrogels is also consistent with previously published literature showing similar elastic recovery during unloading in agarose hydrogels.[38] Taken together, these findings expand our understanding of how chondrocyte morphology is altered by mechanical deformation in viscoelastic scaffolds and further elucidates how dynamic covalent crosslinks can be used to modulate the cellular response. This information may be relevant for cartilage tissue engineering applications, considering the well-established relationship between chondrocyte morphology and phenotype.[39]

To put the aforementioned findings into greater context for cartilage tissue engineering, we then explored how nascent ECM protein deposition over the first week of culture can influence the transmission of compressive strains within CAN networks. (Fig. 4) We observe that chondrocytes rapidly begin to synthesize ECM molecules in these hydrogel constructs, potentially influencing the local presentation of biomechanical cues.[40] Here, CAN-chondrocyte hydrogels were cultured at 37°C with 5% CO_2 in chondrocyte growth medium for 1 week. Representative histology sections stained for sulfated glycosaminoglycans (sGAGs) show variations in the spatial distribution of deposited matrix as a function of viscoelastic creep. (Fig. 4A) In the most adaptable hydrogels, (100%) cell secreted sGAGs were distributed a larger distance from the chondrocytes, which was similarly observed in the 78% CANs. Interestingly, many cells in the fully adaptable 100% viscoelastic CANs appeared in lacunae often with more than one chondrocyte. In contrast, the elastic hydrogels (0%) constrained deposited sGAGs with sharply defined boarders at the hydrogel-neotissue interface.[26] For cartilage tissue engineering, scaffolds must act in concert with the kinetics of tissue growth to allow neotissue percolation, ultimately replacing the scaffold with ECM.[41] In this respect, adaptablility of the viscoelastic CANs (100% and 78%) allows for a greater degree of cell-secreted matrix integration. This suggests that viscoelastic creep of dynamic covalent crosslinks could be a viable mechanism for improving cartilage tissue engineering without compromising mechanical properties of tissue engineering matrices.

To interpret how differences in pericellular matrix deposition might influence chondrocyte behavior, chondrocyte-laden hydrogels were similarly subjected to a compressive strain and imaged before (0% strain) and during deformation (20% strain). Deformation index was normalized to better represent the transmission of compressive strain in different conditions by accounting for minor deviations in unstrained chondrocyte morphology during extended culture. The results show that pericellular matrix deposition reduced cellular deformation in viscoelastic CANs, implying that chondrocytes can remodel the cellular microenvironment in a way that protects chondrocytes from compressive strains. (Fig. 4B) This pericellular matrix-mediated strain protection has been examined extensively by Knight et al. where hyaluronidase treatment was used to degrade sGAGs, restoring the magnitude of chondrocyte deformation at day three to that of day one.[34,42] In this work, the effect was more significant in the 78% hydrogels than the most viscoelastic 100% hydrogels despite more matrix deposition in the latter case. We hypothesized that this observation

may be the result of enhanced proliferation in the highly adaptable 100% hydrogels that complicates the analysis. To test this, we assumed a uniform cell distribution and calculated the approximate number of chondrocytes in each hydrogel using 3D reconstructions from confocal microscopy images. (Fig. 4C & S5) We found that both networks containing percolating benzyl-hydrazone crosslinks (78% & 0%) showed similar chondrocyte densities relative to initial seeding density (5×10^6 cells/mL) which implies that little or no proliferation was possible in these networks after only one week. In contrast, the total number of chondrocytes roughly doubled in highly viscoelastic 0% hydrogels, despite variable results between hydrogel replicates. ($P \leq 0.1$)

To further gauge the implications of viscoelastic differences for cartilage tissue engineering, 1-week samples were collected after 6 hours of deformation at 20% strain and analyzed for expression of chondrocyte-specific markers using qPCR. We investigated the relative expression ratio of collagen type I (Col1) to collagen type II (Col2) as an established metric for quantifying chondrocyte dedifferentiation.[43] More specifically, native chondrocytes express primarily Col2 in healthy articulating joints, whereas the expression of Col1 is indicative of bias towards a fibrochondrocyte phenotype and the formation of mechanically inferior fibrocartilage.[44] The data shows an interesting trend towards an increase in the ratio of Col1:Col2 expression in highly elastic 0% hydrogels, showing almost and order of magnitude increase compared to the viscoelastic 100% and 78% CANs. These results suggest that viscoelasticity and adaptability of the hydrazone CANs may help to ameliorate the detrimental effects of static deformation on chondrocyte gene expression.[45] (Fig 4D) This mechanism has been previously proposed by Nicodemus & Bryant to explain observed changes in chondrocyte gene expression during dynamic cyclic compression in bioreactor cultures.[46] Future work in this space could investigate physiologically relevant deformation regimes during extended cell culture in bioreactors to build on the fundamental understanding established here.

Conclusion

Joint movement causes deformation of articular chondrocytes and their surrounding matrix *in vivo,* and the morphology changes associated with these events have implications for cartilage tissue engineering.[47] In this work, we establish hydrazone crosslinked PEG hydrogels for studying the effects of viscoelastic rearrangement of covalent crosslinks on chondrocyte function during mechanical deformation. Using *in situ* deformation microscopy, we found that the morphology of encapsulated chondrocytes could be controlled by altering adaptation rates of covalent crosslinks during the application of a physiologically relevant strain. Significantly, these experiments show that chondrocytes are able to exert forces on their surrounding matrix over time, and that dissipative phenomena (*i.e.,* creep compliance & stress relaxation) allow chondrocytes to regain native rounded morphologies under static loads in hydrazone CANs. Viscoelasticity also led to differences in the pericellular distribution of sGAGs after one week, differentially interrupting the biophysical transmission of compressive strain to encapsulated chondrocytes. Finally, viscoelastic creep and pericellular matrix deposition may reduce some of the detrimental effects of static deformation by enabling proliferation and improving the relative expression of collagen type II to collagen type I. These findings provide a basis to inform future work using dynamic

covalent chemistries to design next generation biomaterials for studying and controlling chondrocyte behavior for cartilage tissue engineering.

Supplementary Material

Refer to Web version on PubMed Central for supplementary material.

Acknowledgments

Some graphics were created using BioRender.com. The author's would like to acknowledge the director of the BioFrontiers Advanced Light Microscopy Core, Dr. Joe Dragavon and the instrument shop manager, Dragan Mejic. This work was funded by NIH grants (R01 DK120921 & R01 DE016523). B.M.R. was partially supported by a DoE GAANN Fellowship. C.J.W was supported by NIH Predoctoral Fellowship (F31HL142223).

References

1. Wallace IJ, Worthington S, Felson DT, Jurmain RD, Wren KT, Maijanen H, Woods RJ and Lieberman DE, Proc. Natl. Acad. Sci. U. S. A, 2017, 114, 9332–9336. [PubMed: 28808025]
2. Deshpande BR, Katz JN, Solomon DH, Yelin EH, Hunter DJ, Messier SP, Suter LG and Losina E, Arthritis Care Res. (Hoboken), 2016, 68, 1743–1750. [PubMed: 27014966]
3. B A. and Alice SAR Sophia-Fox J, Sport. Heath, Orthop, 2009, 1, 461–468.
4. Kreulen C, Giza E, Walton J. and Sullivan M, Foot Ankle Spec., 2018, 11, 133–137. [PubMed: 28587484]
5. Kon E, Filardo G, Di Matteo B, Perdisa F. and Marcacci M, Bone Joint Res., 2013, 2, 18–25. [PubMed: 23610698]
6. Bryant SJ and Anseth KS, J. Biomed. Mater. Res, 2002, 59, 63–72. [PubMed: 11745538]
7. Huey DDJ, Hu JJC and Athanasiou KAK, Science (80-.)., 2012, 6933, 917–921.
8. Chaudhuri O, Biomater. Sci, 2017, 5, 1480–1490. [PubMed: 28584885]
9. Wang H. and Heilshorn SC, Adv. Mater, 2015, 27, 3717–3736. [PubMed: 25989348]
10. Mak AF, J. Biomech. Eng, 1986, 108, 123–130. [PubMed: 3724099]
11. Freedman BR and Mooney DJ, Adv. Mater, 2019, 31, 1806695.
12. Anderson DE and Johnstone B, Front. Bioeng. Biotechnol, 2017, 5, 76. [PubMed: 29322043]
13. Lee HP, Gu L, Mooney DJ, Levenston ME and Chaudhuri O, Nat. Mater, 2017, 16, 1243–1251. [PubMed: 28967913]
14. Rosales AM, Vega SL, DelRio FW, Burdick JA and Anseth KS, Angew. Chemie Int. Ed, 2017, 56, 12132–12136.
15. Mcbride MK, Worrell BT, Brown T, Cox LM, Sowan N, Wang C, Podgorski M, Martinez AM and Bowman CN, Annu. Rev. Chem. Biomol. Eng, 2019, 10, 175–198. [PubMed: 30883213]
16. Rosales AM and Anseth KS, Nat. Publ. Gr, 2016, 1, 1–16.
17. Zou W, Dong J, Luo Y, Zhao Q. and Xie T, Adv. Mater, 2017, 29, 1606100.
18. McKinnon DD, Domaille DW, Cha JN and Anseth KS, Adv. Mater, 2014, 26, 865–872. [PubMed: 24127293]
19. McKinnon DD, Domaille DW, Brown TE, Kyburz KA, Kiyotake E, Cha JN and Anseth KS, Soft Matter, 2014, 10, 9230–9236. [PubMed: 25265090]
20. Kölmel DK, Kool ET, Kö DK, Kool ET, Kölmel DK and Kool ET, Chem. Rev, 2017, 117, 10358–10376. [PubMed: 28640998]
21. Kalia RT, Jeet; Raines J. Kalia and Raines RT, Angew Chem Int Ed Engl., 2008, 47, 7523–7526. [PubMed: 18712739]
22. McKinnon DD, Domaille DW, Cha JN and Anseth KS, Chem. Mater, 2014, 26, 2382–2387.
23. Oommen OP, Wang S, Kisiel M, Sloff M, Hilborn J. and Varghese OP, Adv. Funct. Mater, 2013, 23, 1273–1280.

24. Wang H, Zhu D, Paul A, Cai L, Enejder A, Yang F. and Heilshorn SC, Adv. Funct. Mater, 2017, 27, 1605609.
25. Tibbitt MW and Anseth KS, Biotechnol. Bioeng, 2009, 103, 655–63. [PubMed: 19472329]
26. Richardson BM, Wilcox DG, Randolph MA and Anseth KS, Acta Biomater., 2019, 83, 71–82. [PubMed: 30419278]
27. Bryant SJ, Anseth KS, Lee DA and Bader DL, J. Orthop. Res, 2004, 22, 1143–1149. [PubMed: 15304291]
28. Grady ME, Composto RJ and Eckmann DM, J. Mech. Behav. Biomed. Mater, 2016, 61, 197–207. [PubMed: 26874250]
29. Ferry JD, Viscoelastic properties of polymers, 1980.
30. Anseth KS, Bowman CN and Brannon-Peppas L, Biomaterials, 1996, 17, 1647–1657. [PubMed: 8866026]
31. Guilak F, Ratcliffe A. and Mow VC, J. Orthop. Res, 1995, 13, 410–421. [PubMed: 7602402]
32. Bader DL and Knight MM, Med. Biol. Eng. Comput, 2008, 46, 951–963. [PubMed: 18726630]
33. Bryant SJ, Chowdhury TT, Lee DA, Bader DL and Anseth KS, Ann. Biomed. Eng, 2004, 32, 407–417. [PubMed: 15095815]
34. Lee DA, Knight MM, Bolton JF, Idowu BD, Kayser MV and Bader DL, J. Biomech, 2000, 33, 81–95. [PubMed: 10609521]
35. Cameron AR, Frith JE and Cooper-White JJ, Biomaterials, 2011, 32, 5979–5993. [PubMed: 21621838]
36. Knight MM, Van De Breevaart Bravenboer J., Lee DA, Van Osch GJVM, Weinans H. and Bader DL, Biochim. Biophys. Acta - Gen. Subj, 2002, 1570, 1–8.
37. Rubinstein M. and Colby RH, Polymer physics, 3rd edn., 2003.
38. Lee DA and Bader DL, Vitr. Cell. Dev. Biol. - Anim. J. Soc. Vitr. Biol, 1995, 31, 828–835.
39. Hall AC, Curr. Rheumatol. Rep, 2019, 21, 38. [PubMed: 31203465]
40. Loebel C, Kwon MY, Wang C, Han L, Mauck RL and Burdick JA, Adv. Funct. Mater, 2020, 1909802.
41. Vernerey FJ and Bryant S, Curr. Opin. Biomed. Eng, 2020, 15, 68–74.
42. Knight MM, Lee DA and Bader DL, Biochim. Biophys. Acta - Mol. Cell Res, 1998, 1405, 67–77.
43. Marlovits S, Hombauer M, Truppe M, Vècsei V. and Schlegel W, J. Bone Joint Surg. Br, 2004, 86, 286–95. [PubMed: 15046449]
44. Benjamin M. and Ralphs JR, Int. Rev. Cytol, 2004, 233, 1–45. [PubMed: 15037361]
45. Nicodemus GD and Bryant SJ, Osteoarthr. Cartil, 2010, 18, 126–137.
46. Nicodemus GD and Bryant SJ, J. Biomech, 2008, 41, 1528–1536. [PubMed: 18417139]
47. Gilbert SJ and Blain EJ, in Mechanobiology in Health and Disease, 2018, pp. 99–126.

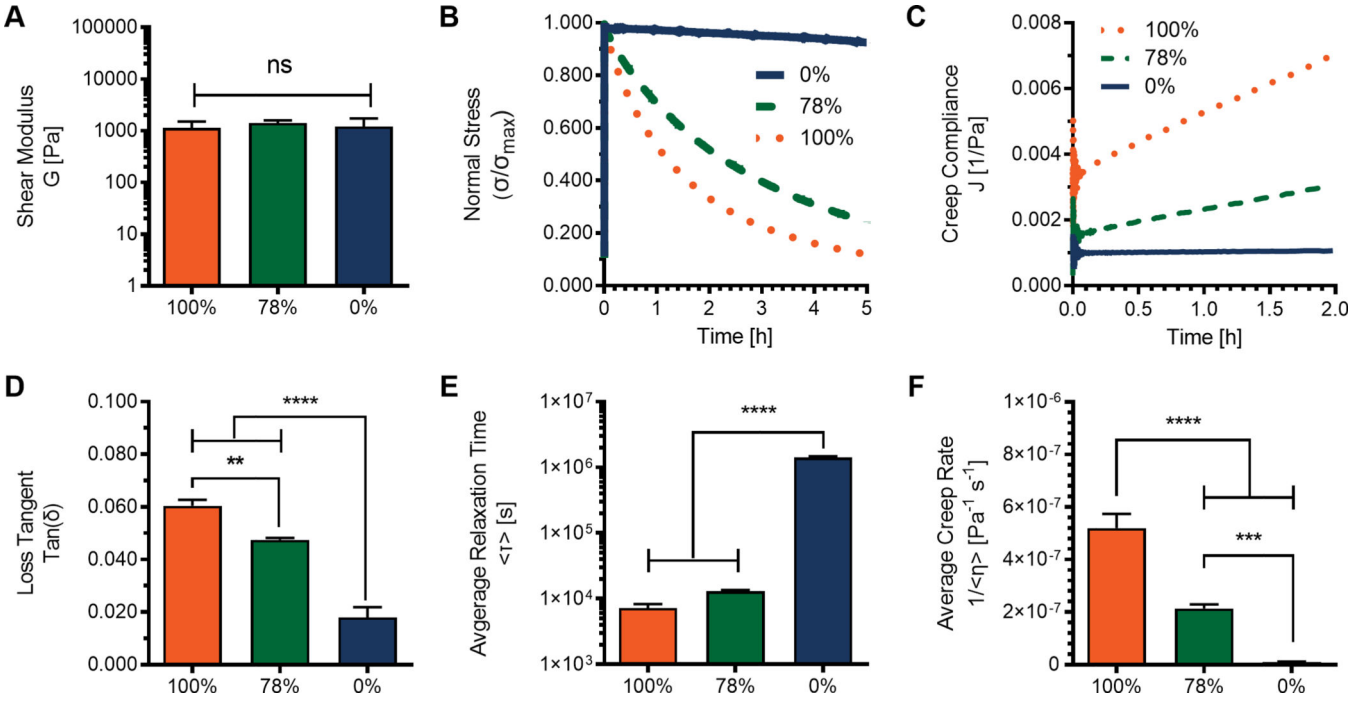

Fig. 1.

Rheological testing to investigate the viscoelastic/elastic material properties stemming from differences in chemical equilibria of dynamic hydrazone crosslinks. Off-stoichiometry (r = 0.8) hydrogels (~3wt%) were formed in situ between parallel plates using reactive 8-arm 10kD PEG macromers. A) Shear moduli were calculated $G = [(G')^2 + (G'')^2]^{1/2}$ using plateau values ($dG'/dt \approx dG''/dt \approx 0$) measured by time sweep during gelation *in situ* at 1% strain and 1 rad/s. B) Stress relaxation of a 10% strain monitored as a function of time. C) Creep compliance measured over time by the application of a constant 100 Pa stress. D) Loss tangents (tan(δ)) were calculated as the quotient of storage and loss moduli at 1% strain and 0.05 rad/s. E) Average relaxation times (<τ>) calculated based on the Kohlrausch–Williams–Watts stretched exponential function. F) Linear average creep rates (<1/η>) were fit to data excluding initial creep ringing. Data represent the average of measurements made in triplicate (n=3), with standard deviations where applicable. Significance represents the results of one-way ANOVA with Tukey's multiple comparisons test showing $P \geq 0.05$ = ns, $P < 0.05$ = *, $P < 0.01$ = **, $P < 0.001$ = ***, $P < 0.0001$ = ****.

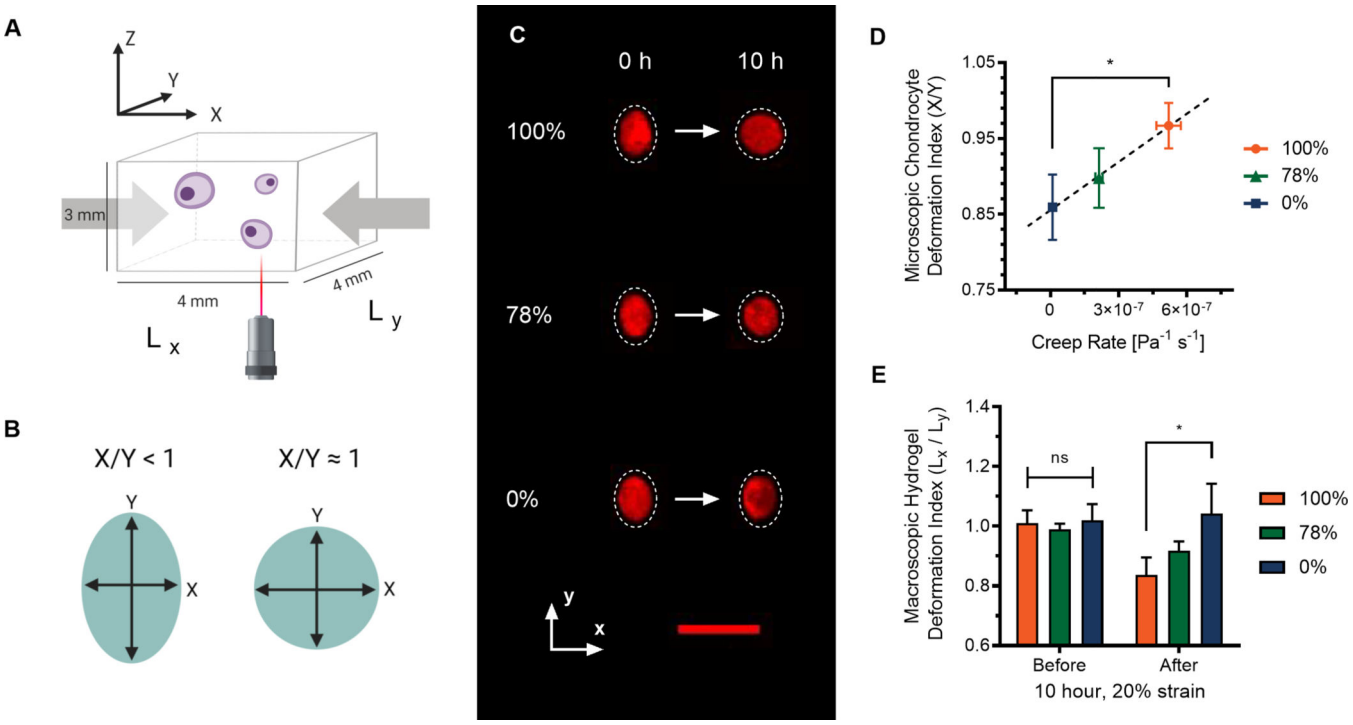

Fig. 2.

Viscoelastic creep compliance influences chondrocyte morphology during deformation. Viscoelastic alkyl-hydrazone hydrogels demonstrate both macroscopic and microscopic time-dependent material deformation. A) Schematic illustrating the experimental setup and hydrogel dimensions. B) Schematic illustrating how chondrocyte deformation index (X/Y) is measured. C) Chondrocytes stained with CellTrackerTM Orange and imaged in situ during deformation by confocal microscopy. Images represent maximum intensity projections illustrating changes in chondrocyte morphology over 10 hours of compressive loading at 20% strain. Scale bar represents 30 μm. D) Correlation between microscopic chondrocyte deformation indexes and viscoelastic creep rates of hydrazone hydrogels after 10 hours of 20% strain. E) Macroscopic deformation indexes before and after loading. Significance represents one-way or two-way ANOVA with Tukey's and Sidak's multiple comparisons tests, $P \geq 0.05$ = ns, $P < 0.05$ = *.

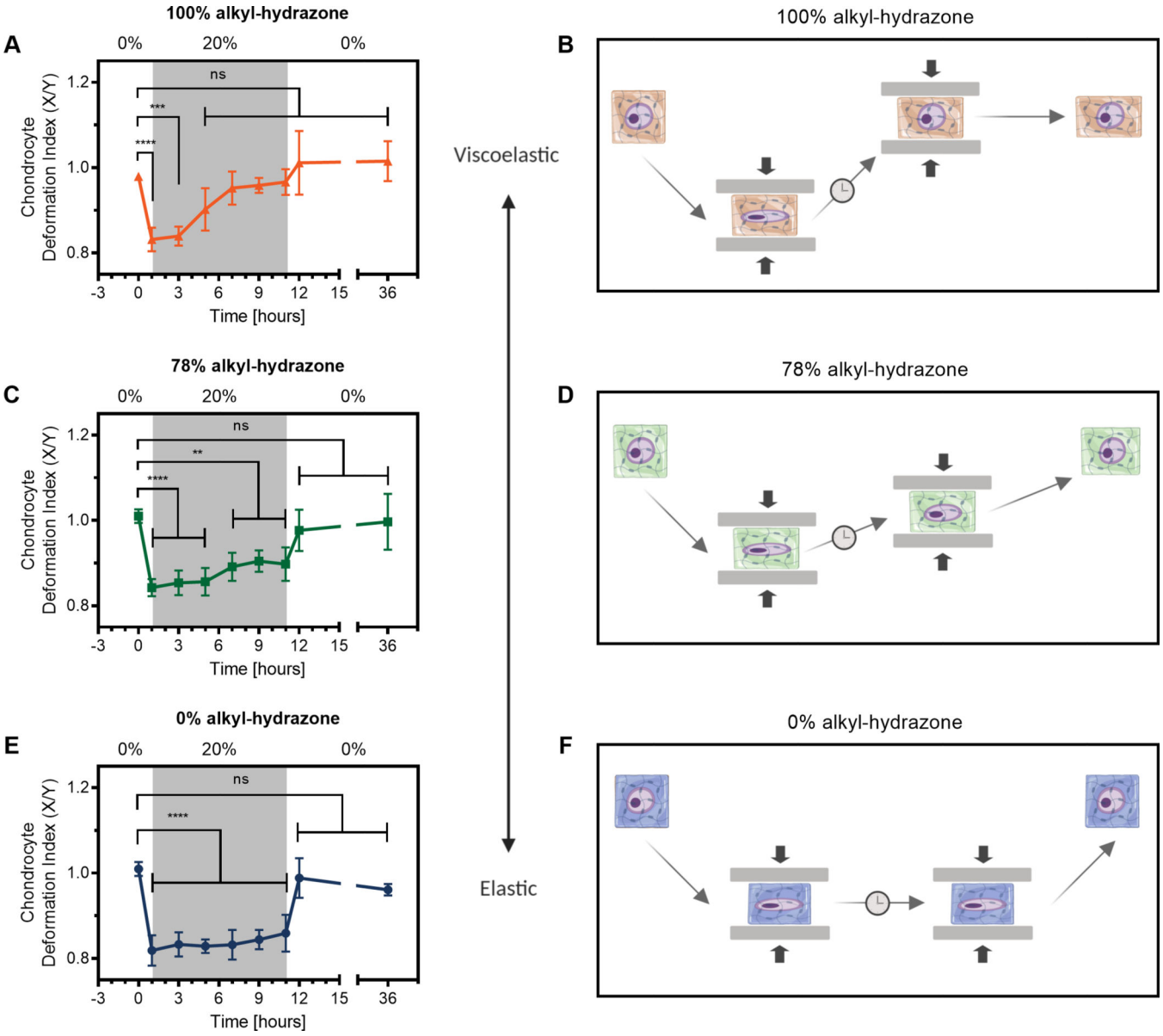

Fig. 3.

Viscoelastic and elastic hydrazone CANs impart biophysical cues to encapsulated chondrocytes differently over time during mechanical deformation. A), C), and E) show deformation indexes graphed over time. Grey regions represent 10 hours chondrocyte-laden hydrogels were subjected to a 20% uniaxial compressive strain. Data represent the mean and standard deviation of three hydrogels (n=3), where morphology data from 300 cells were averaged. Significance represents the results of two-way ANOVA with Dunnett's multiple comparisons test showing $P \geq 0.05$ = ns, $P < 0.05$ = *, $P < 0.01$ = **, $P < 0.001$ = ***, $P < 0.0001$ = ****. B), D), and F) are schematics illustrating changes in chondrocyte morphology due to viscoelastic/elastic material properties to aid in the interpretation of deformation index data.

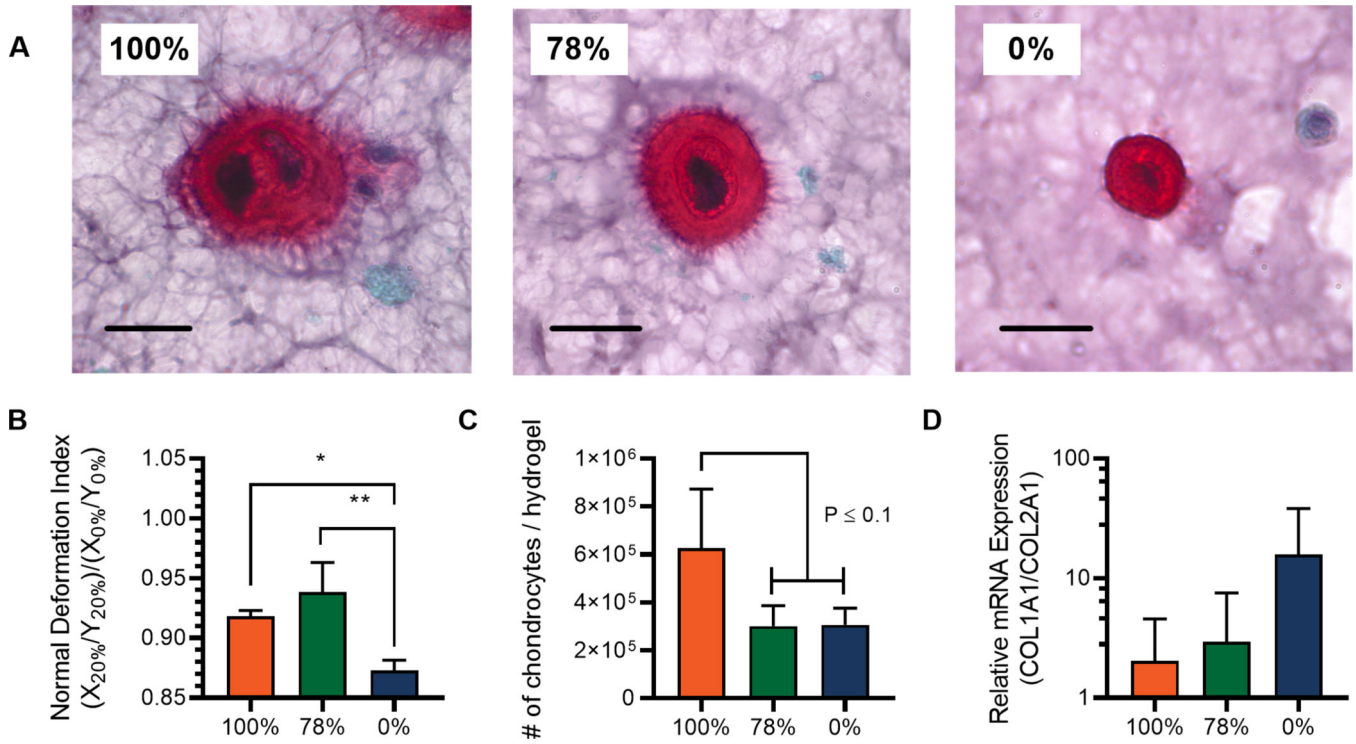

Fig. 4.

Pericellular matrix deposition in viscoelastic hydrazone hydrogels influences the transmission of biophysical cues. Tissue engineering is a dynamic process and chondrocytes deposit extracellular matrix over time to influence the mechanics of their own microenvironments. A) Histological sections stained with Safranin O. sGAGs are represented by the red stain area with nuclei stained violet/black. Scale bars represent 20 μm. B) Quantification of normalized deformation index (X20% / Y20%) / (X0% / Y0%) after one week of culture illustrates differences in the transmission of a 20% strain to encapsulated chondrocytes. C) Estimation of the number of chondrocytes per hydrogel extrapolated from confocal microscopy data showing increased cell populations in the absence of percolating elastic networks of stable benzyl-hydrazone crosslinks. D) Relative expression of Col1 and Col2 after 6 hours of loading at 20% strain, normalized by GAPDH expression. The trend suggests that ECM disposition in viscoelastic CANs can help mitigate negative effects of static loading.